Conformationally Locked Heterocycles. Structure of a Doubly Bridged Pyrimido[1,2-*a*]pyrimidine from the Hantzsch Synthesis with 4-(2-Hydroxyphenyl)but-3-en-2-one

Jan Světlík*

Department of Analytical Chemistry, Faculty of Pharmacy, Comenius University, Odbojarov 10, 832 32 Bratislava, Slovak Republic

Tibor Liptaj

NMR Laboratory, Slovak Technical University, Radlinskeho 9, 812 37 Bratislava, Slovak Republic

František Tureček*

Department of Chemistry, Bagley Hall, Box 351700, University of Washington, Seattle, WA 98195-1700 USA

Received May 21, 1998
Revised December 3, 1998

1D and 2D nmr spectroscopy was used to assign the structure to the minor product from cyclocondensation of 4-(2-hydroxyphenyl)but-3-en-2-one with cyanamide, which was identified as (6*R**, 9*R**, 15*R**, 17*R**)-6,9-dimethyl-6,17:9,15-dimethano-6*H*,15*H*,17*H*-[1,3,5]benzoxadiazocino[4,5-*d*][1,3,5]benzoxadiazocine-7(9*H*)-carbonitrile, a doubly oxygen-bridged pyrimido[1,2-*a*]pyrimidine derivative. The observed stereoselectivity and reaction mechanisms are discussed with the help of molecular mechanics and semi-empirical PM3 calculations.

J. Heterocyclic Chem., **36**, 209 (1999).

We have reported previously that Hantzsch condensations with 4-(2-hydroxyphenyl)but-3-en-2-one (**1**) yielded oxygen-bridged tetrahydropyridines and tetrahydropyrimidines [1]. In particular, condensation of **1** with cyanamide produced tetrahydropyrimidine **2** accompanied by its isomer **3**, which both corresponded to adducts of **1** with two equivalents of cyanamide (Scheme 1). In addition, a 2:2 adduct was isolated ($C_{22}H_{20}N_4O_2$) whose structure was tentatively assigned on the basis of mass and one-dimensional nmr spectra as one of the four hexacyclic, doubly bridged isomers, *e.g.*, *cis-anti*-**4**, *cis-syn*-**4**, *trans-anti*-**4**, or *trans-syn*-**4**, (Scheme 2). We now provide spectral and computational evidence that points to the *cis-anti*-**4** structure for the product of the Hantzsch synthesis.

Results and Discussion.

Compound **4** was formed when cyclocondensation of **1** and cyanamide was carried out in warm or refluxing methanol or ethanol, which also produced **2** and **3**. The low yield of **4** reported previously (4%) [1] was now improved to 16% by conducting the condensation in methanol at room temperature for several days. This allowed us to obtain sufficient quantities of **4** for 2D-nmr studies. The purity of crystalline **4** was confirmed by its ^{13}C-nmr spectrum, which showed all twenty-two ^{13}C signals resolved [1]. Unfortunately and in spite of numerous attempts, we were unable to grow a suitable crystal for X-ray analysis.

Scheme 1

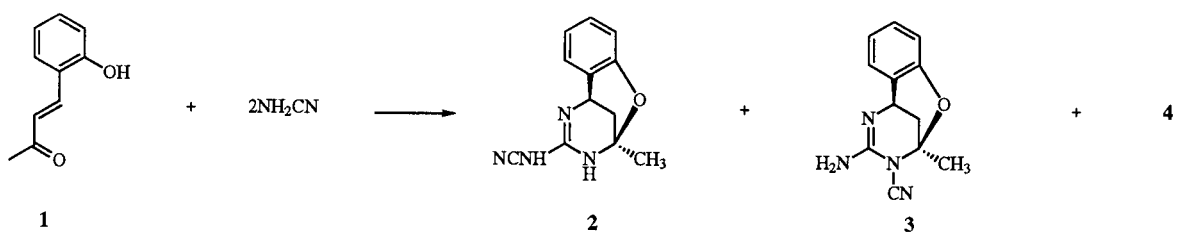

1 2 3

Scheme 2

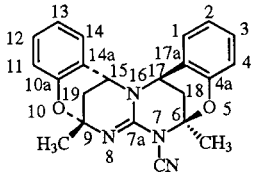

cis-anti-**4**

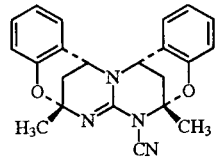

cis-syn-**4**

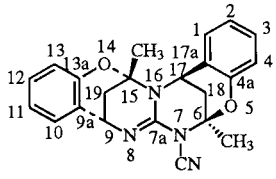

trans-anti-**4**

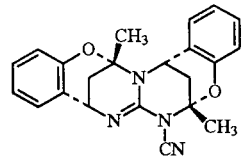

trans-syn-**4**

The structures for **4** correspond to various regio- and stereochemical combinations in the condensation of **1** with cyanamide. All four structures contain the same building blocks that are arranged in a head-to-head (*cis-anti*-**4** and *cis-syn*-**4**) or head-to-tail (*trans-anti*-**4** and *trans-syn*-**4**) fashion and lack symmetry due to the presence of the nitrile group. Inspection of models showed some distinguishing structural features that could be probed by nmr spectroscopy. In particular, *trans-anti*-**4** has the bridgehead methines (C-9 and C-17) on the opposite sides and faces of the pyrimido[1,2-*a*]pyrimidine skeleton, which should prevent Nuclear Overhauser Effect (NOE) to be observed between H-9 and H-17. The *trans-syn* isomer also has the H-9 and H-17 protons on the opposite sides of the skeleton; therefore a very weak (if any) NOE enhancement could be expected for the remote bridgehead protons. Note that the pyrimido[1,2-*a*]pyrimidine skeleton is made rigid by the presence of the C=N double bond and double bridging. By contrast, the head-to-head structures (*cis-anti*-**4** and *cis-syn*-**4**) have the bridgehead methines (H-15 and H-17) in closer proximity. ^1H-^1H dipole-dipole interaction between H-15 and H-17 was confirmed by 1D differential NOE [2], which showed significantly enhanced intensities for both H-15 (6%) and H-17 (7%) signals upon irradiating the other proton frequency (Table 1). These measurements allowed us to safely exclude the head-to-tail isomers and focus our attention to distinguishing *cis-anti*-**4** and *cis-syn*-**4**.

Table 1

NMR Spectroscopic Parameters of *cis-anti*-**4** [a]

Atom	δ_C	δ_H	J(H,H)		H,C^{n}J-corr [b]	H,H-NOE [b,c]
1	128.5	7.69	1, 2: 7.6	1, 3: 1.6	3, 4a, 17	2(14), 15(4), 17(6),
2	122.4	7.07	2, 3: 7.2	2, 4: 1.1	4, 4a, 17a	
3	130.1	7.32	3, 2: 7.3	3, 1: 1.8	1, 4a, 17a	
4	117.0	6.96	4, 3: 8.3	4, 2: 0.8	2, 4a, 17a	
4a	149.7					
6	86.0					
6-CH_3	25.3	1.80			6, 18	4(<0.5), 18(1)
7a	145.4					
9	83.2					
9-CH_3	28.7	1.47			9, 19	11(<0.5), 19(1)
10a	152.2					
11	116.6	6.78	11, 12: 8.0	11, 13: 1.0	10a, 13, 14a	
12	129.5	7.20	12, 13: 7.5	12, 14: 1.8	14, 10a	
13	120.0	6.90	13, 12: 7.3	13, 11: 1.1	11, 14a	
14	128.3	7.57	14, 13: 7.5	14, 12: 1.6	10a, 12, 15	13(16), 15(6), 17(3)
14a	122.9					
15	51.2	5.08			7a, 9, 10a, 14 14a, 17, 19	1(3), 14(5), 17(6), 19(1)
17	49.0	4.72			1, 4a, 7a	1(5), 14(2), 15(7), 18(1)
17a	122.4					
18_{ax}	32.5	2.05	18_{ax}, 18_{eq}: 13.9 18_{ax}, 17: 2.9		6, 17, 17a	
18_{eq}	32.5	2.41	18_{eq}, 18_{ax}: 13.9 18_{eq}, 17: 3.4		6, CN	
19_{ax}	32.0	1.52	19_{ax}, 19_{eq}: 13.2 19_{ax}, 15: 3.3		9, 14a, 15	
19_{eq}	32.0	2.07	19_{eq}, 19_{ax}: 13.2 19_{eq}, 15: 2.5		9	
CN	107.5					

[a] Chemical shifts (δ scale) in ppm, coupling constants (J) in Hz; [b] Correlation with proton indicated in the first column; [c] NOE signal enhancements (%).

To highlight the structural differences between the head-to-head isomers we carried out molecular mechanics (MM2) [3] and semi-empirical PM3 [4] calculations. MM2 calculations used a fixed set of standard bond lengths while the bond and dihedral angles were optimized within an empirical force field [3]. This approach was deemed to be adequate for the relatively rigid skeletons of *cis-anti*-**4** and *cis-syn*-**4**. PM3 calculations used full geometry optimization including all bond lengths and can be expected to provide reasonable estimates of equilibrium geometries and relative enthalpies for the molecules under study. The PM3-optimized structures are shown in Figure 1 while the relevant geometry parameters are listed in Table 2. Both PM3 and MM2 structures showed differences in the interatomic distances between the bridgehead protons (H-15, H-17) and several other protons in *cis-anti*-**4** and *cis-syn*-**4**. In particular, H-15 was in close proximity to H-17 (2.34 Å) and H-14 (2.46 Å), H-17 was close to H-1 (2.46 Å), and H-1 was close to H-14 (1.8 Å) in *cis-syn*-**4** (Figure 1). In contrast, the internuclear distances between H-1 and H-15 (3.22 Å) and H-17 and H-14 (3.18 Å) were long in *cis-syn*-**4**; *cis-anti*-**4** showed H-15 and H-17 within 2.45 Å, which distance was slightly longer than that in *cis-syn*-**4**. Quite predictably, H-1 and H-14 were mutually remote (3.84 Å) in *cis-anti*-**4**. However, H-1 and H-15 (2.89 Å) and especially H-14 and H-17 (2.29 Å) were spatially close. Qualitatively similar conclusions also followed from MM2 calculations, which showed somewhat shorter interproton distances because of the shorter standard C-C and C-N bond lengths used.

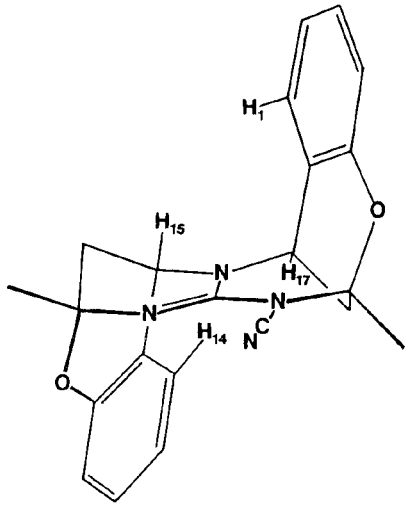

cis-anti-4

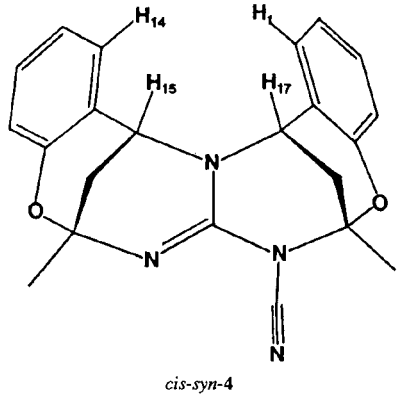

cis-syn-4

Figure 1. PM3 optimized geometries of *cis-anti*-**4** and *cis-syn*-**4**. The bond lengths and angles are in Table 2.

It is also worth noting that both PM3 and MM2 predicted *cis-anti*-**4** to be more stable than *cis-syn*-**4**. The PM3 energy difference (7 kJ mol^{-1}) was smaller than that from MM2 (14 kJ mol^{-1}), but both would predict *cis-anti*-**4** to predominate in an equilibrated mixture of isomers. The lower stability of *cis-syn*-**4** is probably due to steric repulsion of the aromatic rings, which are placed on the same face of the pyrimido[1,2-*a*]pyrimidine skeleton. The PM3 optimized geometry indicates that the steric repulsion in *cis-syn*-**4** is alleviated by twisting the saturated pyrimidine ring, which removes the parallel stacking of the *syn*-aromatic rings, but introduces additional strain in the heterocycle. No such adjustment is needed in *cis-anti*-**4**. The torsional angles in the saturated pyrimidine ring (in absolute values) differed for *cis-syn*-**4** and *cis-anti*-**4**, *e.g.*, 14 and 39 degrees for the C-6—N-7—C-7a—N-16, 34 and 5 degrees for the C-18—C-6—N-7—C-7a (Table 2), and 47 and 21 degrees for the C-7a—N-16—C-17—C-18 bond systems, respectively.

The short inter-proton distances predicted by the calculations gave rise to dipole-dipole interactions that were observed as peak enhancements in the NOE spectra as summarized in Table 1. The NOE data showed that H-1 interacted with H-2, H-17 and H-15 but not with H-14. Likewise, H-14 interacted with H-13, H-15 and H-17. This was expected for *cis-anti*-**4** but not for *cis-syn*-**4**, which should show a H-1-H-14 interaction instead. The NOE data thus pointed unambiguously to the *cis-anti*-**4** structure for the reaction product.

With the structure of *cis-anti*-**4** being known, it was possible to assign the proton and ^{13}C signals in the nmr spectra, for which we used H, C-COSY (HETCOR) [5,6] and selective INEPT [7] techniques. The molecule of *cis-anti*-**4** poses a particular problem because it is *quasi*-symmetrical in that the "left" and the "right" parts contain similar arrangements of proton and carbon nuclei. The protons of the 18-CH_2 and 17-CH represent an ABX spin system which showed J_{AB}, J_{AX} and J_{BX} coupling constants that were very similar to those of the ABX system of the 19-CH_2 and 15-CH. Likewise, the aromatic protons appear as two overlapping ABCD splitting patterns. The ^1H-^1H couplings were confirmed by H,H-COSY

Table 2

PM3 Structure Parameters for *cis-anti*-**4** and *cis*-syn-**4**

Bond [a]	*anti*	*syn*	Angle [a]	*anti*	*syn*	Dihedral [a]	*anti*	*syn*
7a—16	1.440	1.435	7-7a-16	116.6	118.9	6-7—7a-16	-39.3	-14.5
7a—8	1.306	1.307	8-7a-16	124.4	123.8	9-8—7a-16	4.3	2.9
7—7a	1.443	1.445	6-7-7a	118.0	119.8	18-6—7-7a	-4.6	34.4
6—7	1 513	1.509	7a-8-9	120.7	120.9	19-9—8-7a	-25.5	-25.0
8—9	1.482	1.481	7-6-18	109.9	109.0	15-16—7a-8	-14.5	-13.3
5—CH_3	1.532	1.534	8-9-19	111.4	111.3	17-16—7a-7	30.3	21.1
9—CH_3	1.529	1.530	6-18-17	107.7	107.7	5-6—7-7a	116.0	-88.8
5—6	1.436	1.437	7a-16-15	115.0	116.0	10-9—8-7a	96.2	97.2
9—10	1.443	1.440	7a-16-17	116.3	118.7	CH_3-6—7-7a	-129.0	156.0
6—18	1.540	1.540	7-6-CH_3	113.7	110.4	CH_3-9—8-7a	-149.8	-148.7
9—19	1.543	1.544	8-9-CH_3	109.7	109.4	14a-15—16-7a	-74.4	-74.1
17—18	1.528	1.532	7a-7-CN	117.8	117.1	17a-17—16-7a	-97.8	72.2
15—19	1.532	1.535	7-6-5	104.8	108.0	4a-5—6-7	-83.2	92.8
16—17	1.499	1.490	8-9-10	105.8	106.2	10a-10—9-8	-181.2	-177.4
15—16	1.499	1.498	6-5-4a	116.7	117.1	1-17a—17-16	-87.7	95.6
4a—5	1.380	1.378	9-10-10a	116.6	116.5	14-14a—15-16	-92.6	-96.4
10—10a	1.373	1.373	5-4a-17a	124.1	124.0	H-15—19-8	179.9	-180.1
4—4a	1.402	1.403	10-10a-14a	124.3	124.2	H-17-18—6-7	176.4	-178.1
10a—11	1.405	1.405	10-14a-15	119.3	119.6	H_{ax}-18—17-H	-56.3	-59.8
3—4	1.388	1.387	H-15-16	106.3	106.5	H_{eq}-18—17-H	61.2	57.9
11—12	1.386	1.386	H-17-16	109.0	106.4	H_{ax}-19—15-H	58.7	58.7
2—3	1.393	1.393	H_{ax}-18-6	110.0	110.8	H_{eq}-19—15-H	-59.2	-59.2
12—13	1.394	1.394	H_{eq}-18-6	110.0	110.1	H_{eq}-18—6-7	174.1	179.5
1—2	1.389	1.388	H_{ax}-19-9	110.8	110.8	H_{eq}-19—9-8	175.1	175.6
13—14	1.388	1.388	H_{eq}-19-9	111.0	111.1	NC-7—7a-16	170.7	-163.7
1—17a	1.394	1.394	N≡C-7	179.9	179.7			
14—14a	1.395	1.394	H-1-17a	119.6	119.4			
14a—15	1.504	1.505	H-14-14a	119.7	119.4			
17—17a	1.503	1.504	H-4-4a	120.5	120.4			
10a—14a	1.405	1.405	H-11-10a	120.3	120.2			
4a—17a	1.403	1.403						
7—CN	1.393	1.396						
C≡N	1.162	1.162						
15—H-15	1.117	1.117						
17—H-17	1.119	1.117						
18—H-18_{ax}	1.108	1.108						
18—H-18_{eq}	1.108	1.108						
19—H-19_{ax}	1.107	1.107						
19—H-19_{eq}	1.107	1.107						
C_{ar}—H	1.095	1.095						

[a] Bond lengths in Angstroms, bond and dihedral angles in degrees.

spectrum [5] (Table 1), the 1-D ^{1}H-nmr spectrum of *cis-anti*-**4** is shown in Figure 2. To distinguish the coupling patterns of the left and right parts of the molecule it was necessary to identify at least one ^{1}H or ^{13}C resonance pertinent to the particular pyrimidine ring, and use it as a reference point in constructing the spin-spin connectivity. This critical initial step was achieved by a selective INEPT experiment [7]. Irradiation of the methylene proton at δ_H 2.41 resulted in enhancement of ^{13}C signals of the nitrile and hemiaminal (C-6) carbons in the polarization transfer spectrum. This indicated that the H and C atoms involved belonged to the same *N*-cyanohexahydropyrimidine ring. Moreover, the long-range correlation suggested that the connecting bonds, H-18—C-18—C-6—N-7—CN, must have a planar W arrangement; hence, the δ_H 2.41 proton is equatorial. Irradiation of the other methylene proton (H-18_{ax}) at δ_H 2.05 led to increased ^{13}C intensities of C-6, C-17, and the 17a-ipso aromatic carbon (Table 1). The methine proton from this ABX system showed correlations with two aromatic carbons (C-1 and C-4a), and the central guanidine carbon (C-7a). The methyl protons at δ_H 1.80 were correlated with C-6 and C-18 to pinpoint the position of the particular methyl group. The attachment of this methyl group and the corresponding aromatic ring to the *N*-cyanohexahydropyrimidine ring was thus clearly established.

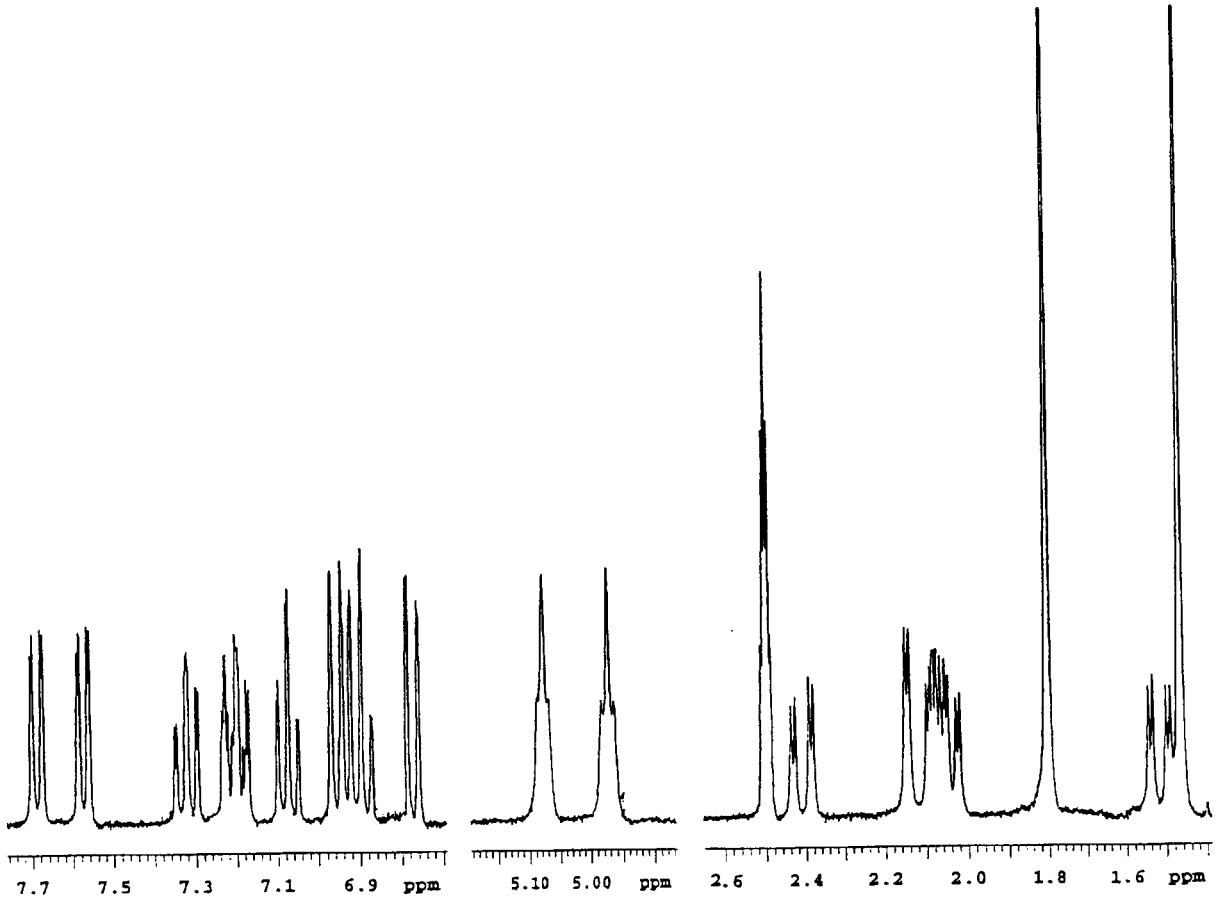

Figure 2. ^{1}H-nmr spectrum of *cis-anti*-**4**. For proton assignments see Table 1.

Additional INEPT data were also collected for the remaining aromatic, methylene and methine protons to complete the connectivity pattern and assign the ^{1}H and ^{13}C signals (Table 1). To finish the nmr characterization of *cis-anti*-**4**, NOE enhancements were determined systematically for all protons in the molecule (Table 1). Interestingly, weak NOE interactions were detected for some relatively remote protons, *e.g.*, 6-CH_3 and H-4, or 9-CH_3 and H-11, which were calculated by PM3 to be 4.65 Å apart. These long distances are at the limit of NOE detection [8]; in the present case NOE may benefit from amplification by magnetization transfer from three equivalent methyl protons. Interestingly, 1D heteronuclear NOE experiments attempting to correlate the methylene and methyl protons with the nitrile ^{13}C nucleus were unsuccessful as no enhancement could be discerned.

The (6*R**,9*R**,15*R**,17*R**)-6,9-dimethyl-6,17:9,15-dimethano-6*H*,15*H*,17*H*-[1,3,5]benzoxadiazocino[4,5-*d*]-[1,3,5]benzoxadiazocine-7(9*H*)-carbonitrile (*cis-anti*-**4**) is the first member of the hitherto unknown family of doubly oxygen-bridged, condensed, polyaza-heterocyclic systems. The compound is formed in a racemic mixture with its enantiomer that differs in the configuration at the C-6, C-9, C-15, and C-17 stereogenic centers. The possible mechanisms of *cis-anti*-**4** formation are shown in Scheme 3. We presume that the cyclocondensation proceeds with bridged tetrahydropyrimidine **3** as an intermediate. Condensation of the latter with **1** can be viewed as a Michael addition of a tautomer of **3** (route *a*, Scheme 3). The stereochemistry of the hydroxyphenyl group is established in this initial step such as to produce an intermediate in which the bulky hydroxyphenyl substituent is exo-oriented with respect to the tricyclic skeleton of **3** for steric reasons. Route *a* is completed by nucleophilic ring closure at the carbonyl group (*d*). This mechanism is analogous to, albeit not identical with that suggested by Wendelin and Harler for the condensation of 1,3-diphenylprop-2-en-1-one with guanidine, which yielded a pyrimido[1,2-*a*]pyrimidine system [9]. An alternative route (*b*, Scheme 3) can be suggested that commences with condensation of the exocyclic amino group in **3** to form a diazatriene intermediate, which subsequently undergoes

1,6-electrocyclization to form the C-15—N-16 bond in the incipient *cis-anti*-**4** (*c*). The latter step is stereogenic and proceeds from the exo-face of the tetrahydropyrimidine ring (Scheme 3). Mechanism *b* has few if any precedents [10] and remains somewhat speculative. The absence of *trans* (head-to-tail) isomers among the isolated products points to the fact that the Michael addition in **1** proceeds primarily by attack of the more nucleophilic ring imine nitrogen in **3**.

Scheme 3

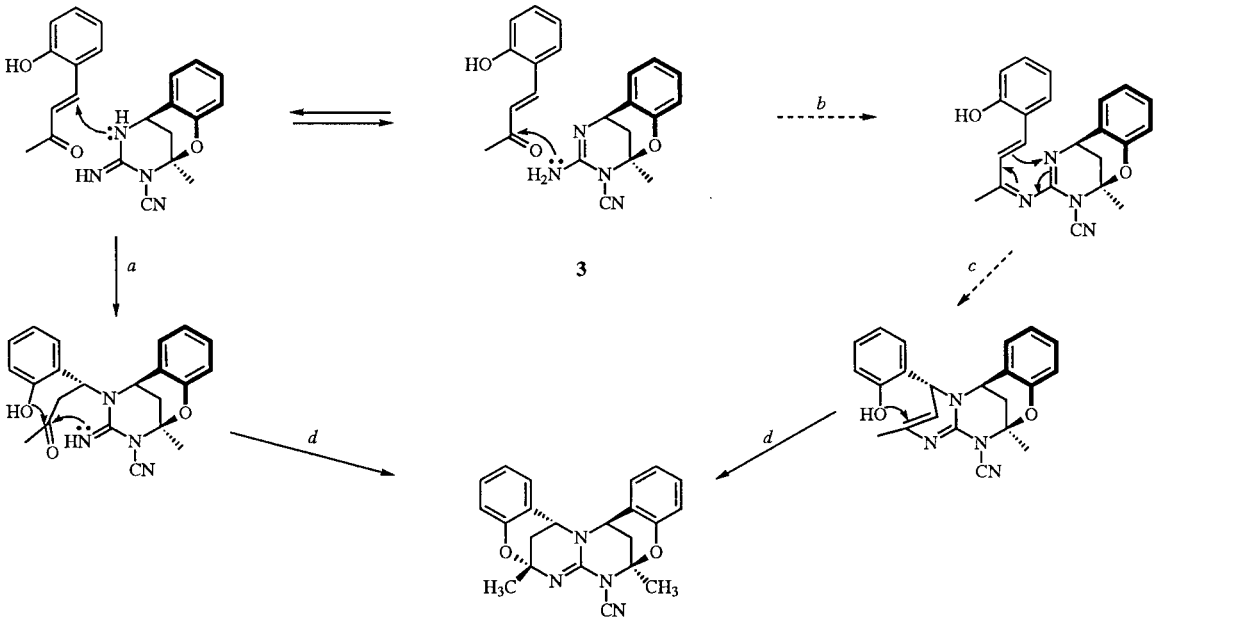

cis-anti-**4**

We finally note that the intermediacy of **2** in the formation of *cis-anti*-**4** cannot be excluded on the basis of product analysis and mechanistic considerations. However, under reaction conditions favoring the formation of **2** over **3**, the yield of *cis-anti*-**4** decreases substantially [1]. This is contrary to what could be expected for a **1** → **2** → *cis-anti*-**4** reaction sequence.

EXPERIMENTAL

The nmr spectra were measured on a Bruker AC 400 instrument equipped with a dual $^1H/^{13}C$ probe operating at 400.136 MHz for ^1H and 100.614 MHz for ^{13}C. The ^1H and ^{13}C chemical shifts were referenced against residual dimethyl-d_6 sulfoxide signals at 2.5 ppm for ^1H and 49.5 ppm for ^{13}C. The ^1H nmr spectral parameters were obtained from a resolution enhanced spectrum with digital resolution of 0.24 Hz/point. The ^{13}C chemical shifts were determined with digital resolution of 0.013 ppm/point. H,H-COSY and HETCOR spectra were acquired using standard pulse sequences provided by the manufacturer. Long-range ^1H-^{13}C correlations were determined using INEPT with spin-selective proton pulses[7] of 15 and 30 ms duration for 90° and 180° angles, respectively. The evolution interval for polarization transfer was set to 50 ms (optimum for $^nJ(^1H$-$^{13}C)$ = 10 Hz), the refocusing period was 40 ms. WALTZ-16 decoupling was employed during acquisition. Steady-state NOE measurements were performed with the pulse program allowing simultaneous NOE determination from several protons. During the saturation interval (6 s) the multiplet of the selected proton was irradiated with a series of line-selective 100-ms pulses which were cycled over all lines in the multiplet. To ensure the same long-term conditions, spectra from each proton irradiation were accumulated step by step in eight scan blocks. Four dummy transients were performed after each change of the irradiated proton to ensure steady-state conditions. A control spectrum with off-resonance irradiation was also acquired. The acquisition time was 1.5 s. NOE enhancements were measured from difference spectra.

The PM3 calculations were carried out with the Gaussian 94 suite of programs [11] on an IBM SP2 cluster. The calculated energies were 0.06789 and 0.06507 hartree (1 hartree = 2625.5 kJ mol^{-1}) for the fully optimized structures of *cis-syn*-**4** and *cis-anti*-**4**, respectively. Harmonic frequency analysis of the PM3 stationary points was not attempted for these large systems.

Improved Preparation of *cis-anti*-**4**.

To a warm solution of butenone **1** (4.86 g, 30 mmoles) in dry methanol (30 ml) was added cyanamide (2.10 g, 50 mmoles) and then 8 drops of piperidine. The reaction mixture was kept at room temperature for 10 days. The crystalline material was filtered, washed with three 5-ml portions of methanol and 10 ml of ether and dried to give 0.9 g (16%) of *cis-anti*-**4**. An analytical sample was recrystallized from methanol; for characterization see reference 1.

Acknowledgments.

J. S. thanks Dr. K. L. Loening, former Nomenclature Director, Chemical Abstracts Service, for his help with naming, numbering and arranging the new heterocyclic system. The computations were conducted using the resources of the Cornell Theory Center that received major funding from the National Science Foundation and New York State with additional support from the Advanced Research Projects Agency, the National Center for Research Resources at the National Institutes of Health, IBM Corporation and members of the Corporate Research Institute.

REFERENCES AND NOTES

[1] J. Světlík, F. Tureček and V. Hanus *J. Chem. Soc., Perkin Trans. 1* 2053 (1988).

[2] M. Kinns and J. K. M. Sanders, *J. Magn. Reson.*, **56**, 518 (1984).

[3] U. Burkert and N. L. Allinger, Molecular Mechanics, American Chemical Society, Washington, DC, 1982.

[4] J. J. P. Stewart, *J. Comput. Chem.*, **10**, 209 (1989).

[5] A. Bax and R. Freeman, *J. Magn. Reson.*, **44**, 542 (1982).

[6] A. Bax and G. Morris, *J. Magn. Reson.*, **42**, 501 (1981).

[7] D. Uhrin and T. Liptaj, *J. Magn. Reson.*, **81**, 82 (1989).

[8] O. Howarth, In Multinuclear NMR, J. Mason, ed, Plenum Press, New York, 1987, p 146.

[9] W. Wendelin and A. Harler, *Monatsh. Chem.*, **107**, 133 (1976).

[10] S. Marchalin and J. Kuthan, *Collect. Czech. Chem. Commun.*, **50**, 1862 (1985).

[11] *Gaussian 94* (Revision D.1), M. J. Frisch, G. W. Trucks, H. B. Schlegel, P. M. W. Gill, B. G. Johnson, M. A. Robb, J. R. Cheeseman, T. A. Keith, G. A. Petersson, J. A. Montgomery, K. Raghavachari, M. A. Al-Laham, V. G. Zakrzewski, J. V. Ortiz, J. B. Foresman, J. Cioslowski, B. B. Stefanov, A. Nanayakkara, M. Challacombe, C. Y. Peng, P. Y. Ayala, W. Chen, M. W. Wong, J. L. Andres, E. S. Replogle, R. Gomperts, R. L. Martin, D. J. Fox, J. S. Binkley, D. J. Defrees, J. Baker, J. P. Stewart, M. Head-Gordon, C. Gonzalez and J. A. Pople, Gaussian, Inc., Pittsburgh, PA, 1995.